Mechanism of Membrane Curvature Induced by SNX1 Insights from Molecular Dynamics Simulations

Liao, Zhenyu; Si, Ting; Kai, Ji-Jung; Fan, Jun

Published in:
The Journal of Physical Chemistry B

Published: 07/03/2024

Document Version:
Post-print, also known as Accepted Author Manuscript, Peer-reviewed or Author Final version

Published version (DOI):
10.1021/acs.jpcb.3c07009

Publication details:
Liao, Z., Si, T., Kai, J.-J., & Fan, J. (2024). Mechanism of Membrane Curvature Induced by SNX1: Insights from Molecular Dynamics Simulations. *The Journal of Physical Chemistry B*, *128*(9), 2144-2153. https://doi.org/10.1021/acs.jpcb.3c07009

Mechanism of Membrane Curvature Induced by SNX1: Insights from Molecular Dynamics Simulations

Zhenyu Liao[1], Ting Si [1,2], Ji-Jung Kai [3,4], Jun Fan[1,3,4] ⋆

[1] Department of Materials Science and Engineering, City University of Hong Kong, Kowloon 999077, Hong Kong, China;

[2] Department of Physics, City University of Hong Kong, Kowloon 999077, Hong Kong, China;

[3] Department of Mechanical Engineering, City University of Hong Kong, Kowloon 999077, Hong Kong, China;

[4] Centre for Advanced Nuclear Safety and Sustainable Development, City University of Hong Kong, Kowloon 999077, Hong Kong, China;

Corresponding Author

⋆ J. Fan: junfan@cityu.edu.hk

Abstract

SNX proteins have been found to induce membrane remodeling to facilitate the generation of transport carriers in endosomal pathways. However, the molecular mechanism of membrane bending and the role of lipids in the bending process remain elusive. Here we conducted coarse-grained molecular dynamics simulations to investigate the role of the three structural modules (PX, BAR and AH) of SNX1 and the PI3P lipids in the membrane deformation. We observed that the presence of all three domains is essential for SNX1 to achieve stable membrane deformation. BAR is capable of remodeling the membrane through the charged residues on its concave surface, but it requires PX and AH to establish stable membrane binding. AH penetrates into the lipid membrane, thereby promoting the induction of membrane curvature; however, it is inadequate on its own to maintain membrane bending. PI3P lipids are also indispensable for membrane remodeling, as they play a dominant role in the interactions of lipids with the BAR domain. Our results enhance the comprehension of the molecular mechanism underlying SNX1-induced membrane curvature and help future studies on curvature-inducing proteins.

Keywords

SNX1, membrane remodeling, scaffolding, PI3P, molecular dynamics simulation

Introduction

Membrane vesicle trafficking is an essential cellular process that involves the cargo transport between membrane-bound organelles within eukaryotic cells.[1] Coat proteins play pivotal roles in the trafficking as they mediate vesicle budding and cargo selection.[2] They can induce the deformation of cell membranes, eventually leading to the release of vesicles. The structures of some coat proteins in vesicle formation, such as COPII, COPI and Clathrin, have been determined to explore how they induce membrane remodeling.[3] As a key component of coat proteins, Sorting nexins (SNX) proteins act a crucial role in endosomal pathways, and dysfunction of SNX proteins is associated with neurodegenerative, cardiovascular and cancerous diseases.[4-8] How SNX proteins bend the membrane to generate the vesicles in the trafficking has attracted great interest.

Sorting nexins (SNX) are a family of proteins characterized by the presence of a phox homology (PX) domain.[9, 10] The PX domain serves as a membrane recruitment module, binding SNX proteins to the endosomal membrane through its special interactions with the endosome-enriched phosphatidylinositol 3-phosphate (PI3P) lipids.[11, 12] Apart from the PX domain, a subset of SNX proteins contains a Bin/amphiphysin/Rvs (BAR) domain, a common building block of membrane-bending proteins. The BAR domain can deform the membrane via a scaffolding mechanism that involves electrostatic interactions between positively charged residues on the concave side of the BAR and the negatively charged lipids.[13-16] Furthermore, the linker region between PX and BAR

can form an amphipathic helix (AH), which is also essential for membrane remodeling.[17, 18] The insertion of AH into the membrane introduces asymmetry between the bilayer, thereby promoting membrane curvature.[19, 20] Experiments have indicated that SNX1 generates membrane curvature through the cooperation of these three structural regions. Pylypenko *et al.* observed that SNX9 approaches the membrane via the PX domain, subsequently inserting AH into the membrane to induce curvature, which is then stabilized by the BAR domain.[18] Zhang et al. showed that SNX1 generates local membrane curvature through PX and AH, while BAR and PX participate in the formation of helical arrays to extend local curvature into global membrane remodeling.[21]

While a general model of SNX-mediated membrane remodeling has been established, molecular details in the bending process remain unclear. It has been found that SNX1 depends on AH to achieve local membrane curvature, whereas the BAR domain does not directly interact with the membrane.[21] However, in some BAR proteins, the BAR domain binds to the membrane and effectively drives membrane deformation through the scaffolding mechanism.[22-24] Therefore, it is necessary to elucidate the role of PX, BAR and AH in driving membrane bending. Another key question is how membrane components influence the generation of membrane curvature. The special interactions between PI3P and SNX proteins are essential for membrane association and further membrane remodeling.[18, 25, 26] How PI3P lipids regulate the membrane sculpting process of SNX1 remains to be determined. Molecular dynamics (MD) simulations

have become a powerful tool for understanding the molecular mechanism of protein-induced membrane curvature.[27, 28] Coarse-grained simulations overcome the limitations of the time and length scale of all-atom simulations and have been extensively employed to elucidate the mechanism of membrane remodeling by BAR[29, 30], ENTH[31], SNF[32] and FAM134B[33] proteins.

Herein, we performed coarse-grained MD simulations to explore the role of the three structural modules and PI3P lipids in the membrane deformation induced by SNX1. To explore the ability of SNX1 to induce membrane tabulation and the underlying mechanism, five independent simulations were conducted, including the full-length SNX1 and the endosomal membrane. Then, these simulations were extended, but only maintaining the AH or BAR domain to distinguish the function of each module in membrane bending. Finally, to probe the influence of lipid composition in the membrane remodeling, a zwitterionic membrane, and an anionic membrane without PI3P, were designed to interact separately with the complete SNX1. Our results indicate that BAR domain, the inserted AH and the PI3P lipids are all essential for membrane remodeling. These simulation findings deepen insights into the molecular mechanism underlying the membrane remodeling induced by SNX1.

Methods

The protein-induced membrane bending is a complex process that may last for several seconds or minutes, making it challenging to simulate.[34] Therefore, we built a nanometer-scale model including a few proteins on the lipid bilayer, aiming to observe the generation of membrane curvature within microseconds (μs). For such a nanoscale system, employing a more precise all-atom simulation would entail high computational costs. As a result, we have opted for widely used coarse-grained MD simulations. Coarse-grained MD simulations were conducted by GROMACS-2020[35] and MARTINI 3[36] force field. The structure of SNX1 was obtained from RCSB protein database, with the PDB code 7D6D (Figure S1). A homodimer was selected from SNX1 lattice as the all-atom model of the protein, and then coarse grained using the martinize 2 script[37]. An elastic network was applied to the protein with a spring constant of 500 kJ/mol and a cutoff distance of 0.9 nm. Side chain corrections were employed. A 42 × 20 nm^2 lipid bilayer model was generated using insane tool[38]. The endosomal membrane is composed of 40% DOPC, 30% DOPE, 20% DOPS and 10% PI3P lipids, consistent with the proportions in the experiment[21]. The parameters for PI3P lipids were obtained from a recent study on the reparameterization of phosphatidylinositide lipids for the Martini 3 force field.[39] The membrane underwent equilibration for 100 ns and then merged with the protein. The SNX1 protein was closely placed above the membrane, with its concave surface facing the membrane. The tips of the BAR domain are positioned at the locations of lipid headgroups to facilitate the rapid establishment of

appropriate contacts between lipids and proteins. The protein and membrane were placed in a 54 × 20 × 20 nm^3 box. The membrane is continuous along the Y-axis while becoming discontinuous along the X-axis (Figure S2). Such membrane ribbon was employed to overcome the repulsive forces from the periodic boundary condition of a simple plane membrane, which has been widely utilized in the membrane remodeling studies.[23, 40-42] The box was solvated in a water box with Martini 3 water beads and then neutralized by adding 150 mM of sodium and chloride ions.

The simulations proceeded with the following steps. First, all systems underwent 10,000 steps of energy minimization, with 1000 $KJ \cdot mol^{-1} \cdot nm^{-2}$ harmonic position restraints applied to both proteins and lipids. Then, the systems were heated to 310K within 2.5 ns under constant temperature/pressure (*NPT*) conditions. Subsequently, a total of 5 ns of equilibration simulations were conducted, gradually reducing the restraints and increasing the time step. Finally, the equilibrated systems underwent 2 μs of production simulations with a time step of 20 fs. In the production simulations, the restrains on lipids were removed, while 200 $KJ \cdot mol^{-1} \cdot nm^{-2}$ position restraints were applied to the beads of the protein backbone to ensure a reasonable membrane conformation of SNX1 and facilitate the stable membrane curvature generation. The temperature of the systems was controlled by a velocity rescale thermostat[43], while the pressure was maintained at 1 bar by anisotropic Parrinello-Rahman babostat[44]. Compressibility was set to 3×10^{-4} bar^{-1} in the z-direction and 0 bar^{-1} along the xy-direction to ensure the constant size of the lipid membrane throughout the simulations.

The off-diagonal compressibility was also set to 0 bar^{-1} to maintain the rectangular shape of the box. The reaction-field method was employed to calculate electrostatic interactions, whereas a 1.1 nm cutoff was applied to treat van der Waals (vdW) interactions. Details of simulations are listed in Table 1. To validate the convergence of simulations and the rationality of simulation setup, additional simulations were performed and the results are summarized in the Supporting Information (section SI-1).

Model visualization and representation were performed in Visual Molecular Dynamics (VMD) software[45]. Membrane curvature, contact and distance were obtained through locally written scripts. Membrane curvature was obtained by projecting the membrane onto the x-z plane and fitting it with the equation of a circle through least-squares fitting.[46, 47] One contact is counted when the distance between two beads is within a cutoff distance of 5.5 Å. In most cases, the distance refers to the z-component between the centers of mass of molecules. The position of the membrane is regarded as the average position of the phosphorus atoms (PO4 beads) in the upper leaflet. Radial distribution function (RDF) was calculated using gmx rdf, and interaction energies were obtained using gmx energy. Statistical significance analysis was performed using the Student's t-test and one-way analysis of variance (ANOVA) in Python.

No.	Protein	(mol fraction) Lipid	Number of beads	Simulation time (μs)	Replicas
1	SNX1	0.4PC/0.3PE/0.2PS/0.1PI3P	203517	2	5
2	PX-AH of SNX1	0.4PC/0.3PE/0.2PS/0.1PI3P	196026		
3	BAR of SNX1	0.4PC/0.3PE/0.2PS/0.1PI3P	196052		
4	None	0.4PC/0.3PE/0.2PS/0.1PI3P	196146		
5	SNX1	PC	229755		
6	SNX1	0.4PC/0.3PE/0.3PS	224937		

Table 1. Summary of coarse-grained MD simulations in the study.

Results

1. SNX1 remodels membranes through scaffolding and helix insertion mechanism

To assess the ability of SNX1 to induce membrane curvature, membrane ribbon simulations of SNX1 and the endosomal membrane were performed. The snapshots demonstrate that SNX1 induces local membrane curvature in all five independent simulations (Figure 1a and Video S1). The x-z positions of membrane midplanes illustrate that SNX1 produces a positively curved membrane in all replicas (Figure 1b). Time evolution of membrane curvature suggests that SNX can quickly induce membrane perturbations (Figure 1c). The membrane transitions from flat to curved within 0.3 μs in most replicas. The membrane curvature remains 0.01-0.02 nm^{-1} throughout the simulations, while the value reaches 0.025 nm^{-1} at the end of simulation #5. These results indicate that the full-length SNX1 homodimer is sufficient for eliciting local membrane curvature.

To understand the mechanism driving the membrane curvature, the interface between SNX1 proteins and the membrane was analyzed. We observed that both the scaffolding mechanism and the helix insertion mechanism are involved in the membrane remodeling process of SNX1. Our simulation results demonstrate that positively charged residues on the concave side of SNX1 attract negatively charged PI3P lipids through electrostatic interactions, thereby scaffolding the membrane into a curvature (Figure 2a). Normalized frequency of contacts between SNX1 and PI3P lipids reveals that R323, R406, R418, K428 and K429 on the concave surface of BAR domain are

found to form firm contacts with PI3P, indicating the important role of crescent-shaped BAR domain in membrane binding and bending (Figure 2b). Electrostatic potential maps suggest that these residues form multiple negatively charged patches on the concave surface, facilitating the attachment to the anionic endosomal membrane to induce positive curvature (Figure S3). In contrast, the convex side mainly consists of positively charged patches, which are less favorable for interactions with endosomal membranes. The distribution of surface charge of SNX1 enables effective membrane localization and subsequent remodeling.

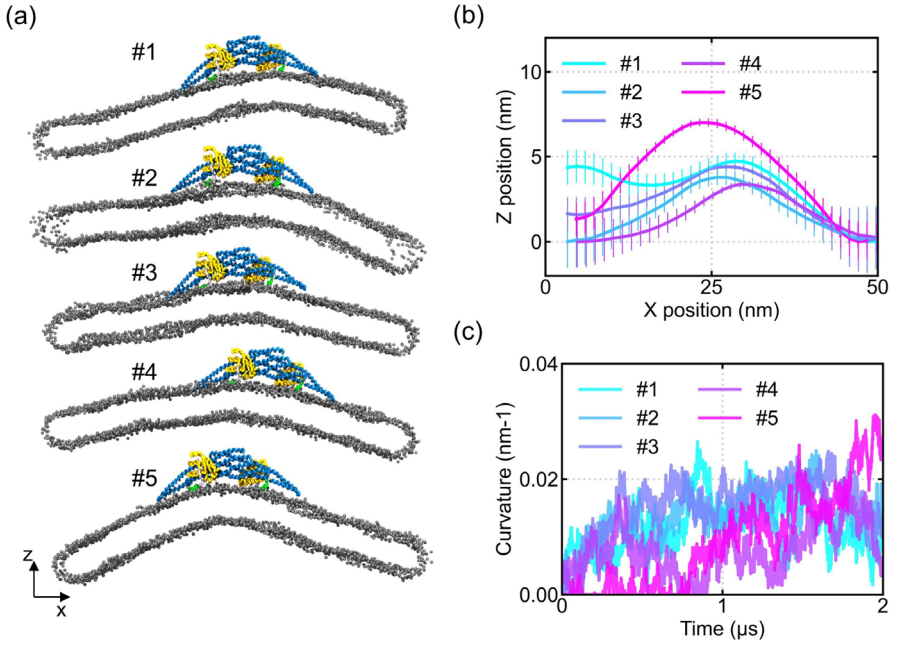

Figure 1. Membrane bending induced by the SNX1 protein. (a) Snapshots of SNX1 inducing membrane curvature from replicas #1 to #5. (b) The z-position of membrane midplanes averaged along the y-direction as a function of the x-position. (c) Time

evolution of membrane curvature. Membrane ribbon simulations demonstrate that the full-length SNX1 can induce local membrane curvature.

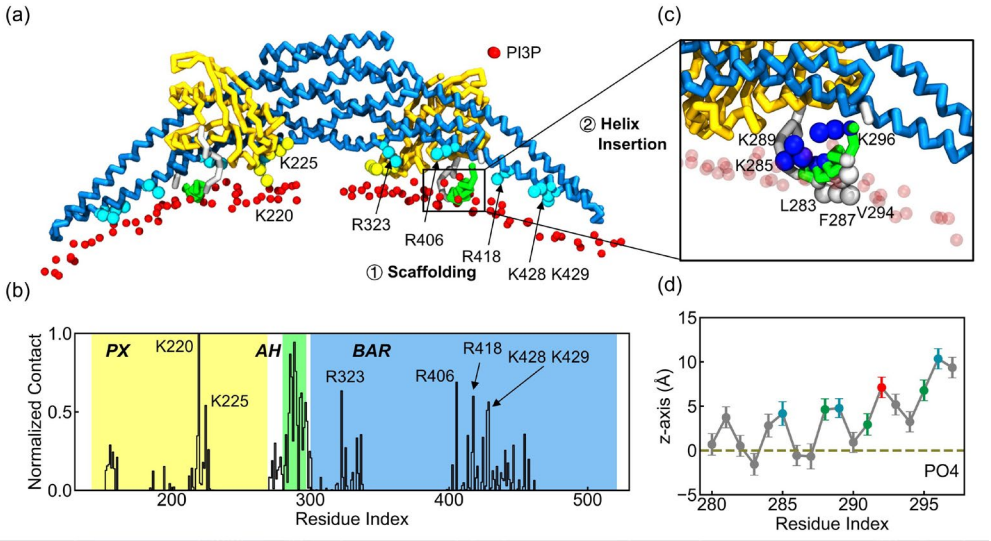

Figure 2. Mechanism of SNX1-induced membrane curvature. (a) Snapshots depicting the interface between SNX1 and PI3P lipids. Residues with stable contacts with PI3P lipids are shown in cyan and yellow spheres, while PI3P lipids in the vicinity of SNX1 are represented by red spheres. (b) Normalized frequency of contacts of SNX1 with PI3P. One contact is counted if the residue is within a 5.5 Å cutoff distance of PI3P lipids in one frame. Normalized contact is calculated by dividing the total contacts for each residue by the total contacts for the residues with the most contacts. (c) Zoomed-in view of the penetration of AH into the membrane. The hydrophobic and charged residues on AH are denoted by white and blue spheres. (d) The penetration depth of individual residues of AH into the membrane. Non-polar, polar, positively charged and negatively charged residues are colored in gray, green, blue and red. The plane of PO4

beads on the upper layer is regarded as the membrane periphery, highlighted by a brown dotted line. SNX1 deforms the membrane through the positively charged residues located on the curved surface of the BAR domain and the embedded AH.

In addition, the helix insertion mechanism also contributes to SNX1-mediated membrane bending. Snapshots of the interface between AH and membranes reveal that hydrophobic residues (L283, F287 and V294) penetrate into the membrane, while charged residues (K285, K289 and K296) stay at the surface of the membrane (Figure 2c). Figure 2d demonstrates that hydrophobic residues have a deeper insertion into the membrane than charged residues, and several hydrophobic residues are buried into the hydrophobic area of lipids (below the PO4 beads). The insertion of AH into the membrane is also verified by the stable contacts between AH and PI3P lipids (Figure 2b). Time evolution of the position of AH relative to the membrane was also calculated (Figure S4). The results show that AH gradually approaches the membrane and reaches a position around 4 Å away from the membrane, with its hydrophobic side facing downward and inserting into the membrane. The PX domain can facilitate the binding of SNX1 to the membrane, by making stable contacts with PI3P lipids via K220 and K225 (Figure 2a and b). Although K225 is believed to participate in the binding pocket of PI3P, snapshots in the simulation show that PI3P lipids do not enter the pocket but only form electrostatic interactions (Figure S5).

The calculation of normalized contact number and interaction energy confirms the involvement of all three structural regions (PX, AH, and BAR) in interactions with the

membrane and provides more details (Figure S6). The normalized contact number demonstrates that PX and BAR exhibit similar probabilities of interacting with the membrane. This suggests that these two domains are anchored to the membrane through non-special charged residues, rather than relying on specific lipid-binding sites. Due to AH being embedded within the lipid bilayer, it has a higher normalized contact number, with over half of its residues in contact with the membrane. The calculation of interaction energy also indicates that, despite AH having only one-tenth the number of atoms compared to BAR, AH (-586.7 KJ/mol) and BAR (-570.3 KJ/mol) show comparable binding strength with the lipid membrane, highlighting the pivotal role of AH in membrane interactions. The averaged interaction energy of PX with the membrane is -293.7 KJ/mol. Considering PX has only about half the number of atoms as BAR, this further demonstrates that PX and BAR exhibit a similar level of affinity to the membrane. These analyses also explain the differences in membrane curvature among different replicas. Replica #5 exhibits the highest membrane curvature induced by SNX1. We observed that in the replica, AH of SNX1 has the largest contact number and maximum interaction energy with the membrane.

Based on these results, we conclude that the full-length SNX1 can bind to the endosomal membrane and induce local membrane curvature. The scaffolding mechanism of BAR domain and the insertion of AH both contribute to membrane deformation.

2. BAR or AH alone struggles to maintain the membrane curvature

Although we have demonstrated that both the scaffolding and helix insertion mechanism occur in the SNX1-induced membrane remodeling, it remains unclear which mechanism dominates in the bending process. To clarify the role of BAR and AH in driving membrane bending, we extended simulations with the full-length SNX1 to simulations with only the BAR domain or AH domain. The BAR-only and AH-only simulations start from the final conformation of the simulation containing the full-length SNX1, where the membrane begins in a bent conformation, and the protein retains only the BAR or AH component, respectively. In the AH-only simulations, the PH domain was also included to facilitate the embedding of AH within the membrane. The presence of PH does not affect the membrane remodeling driven by the helix insertion mechanism, because PX domain only targets PI3P lipids for membrane binding but does not directly participate in membrane remodeling.[21, 26] Moreover, we removed proteins and performed simulations on the membrane that had been curved by the complete SNX1 to validate the ability of SNX1 to induce membrane curvature.

The results indicate that only the BAR domain struggles to maintain the membrane curvature (Figure 3a, S7a and Video S2). The curved membranes become flat in replicas #1, #3 and #4. Similarly, AH alone also has difficulty in keeping the membrane curvature (Figure 3b, S7b and Video S3). Except for replicas #1 and #4, the membrane in other replicas relaxes to a flat conformation. We compared the averaged membrane curvature in the system of the full-length SNX1, BAR only and AH only (Figure 3c).

In the complete SNX1 system, the membrane gradually develops a positive curvature, reaching a curvature of 0.015 nm^{-1}. When the complete SNX1 is removed, the curved membranes flatten out in all replicas, demonstrating the essential role of the complete SNX1 in driving membrane curvature (Figure S7c, S8 and Video S4). When AH or BAR domain is removed, the membrane curvature also undergoes a decrease (Figure 3c). The averaged membrane curvature for both systems gradually decreases from 0.018 nm^{-1} and reaches approximately 0.010 nm^{-1} by the end of the simulations. The curvature distribution reveals that the membrane curvature induced by SNX1 is concentrated around 0.014 nm^{-1}, with no curvature approaching 0 nm^{-1} in any of the replicas, providing evidence that SNX1 can induce membrane remodeling in all replicas (Figure 3d). In contrast, the membrane curvature is smaller in the AH system, whereas many membranes in the BAR system have a curvature of 0 nm^{-1}.

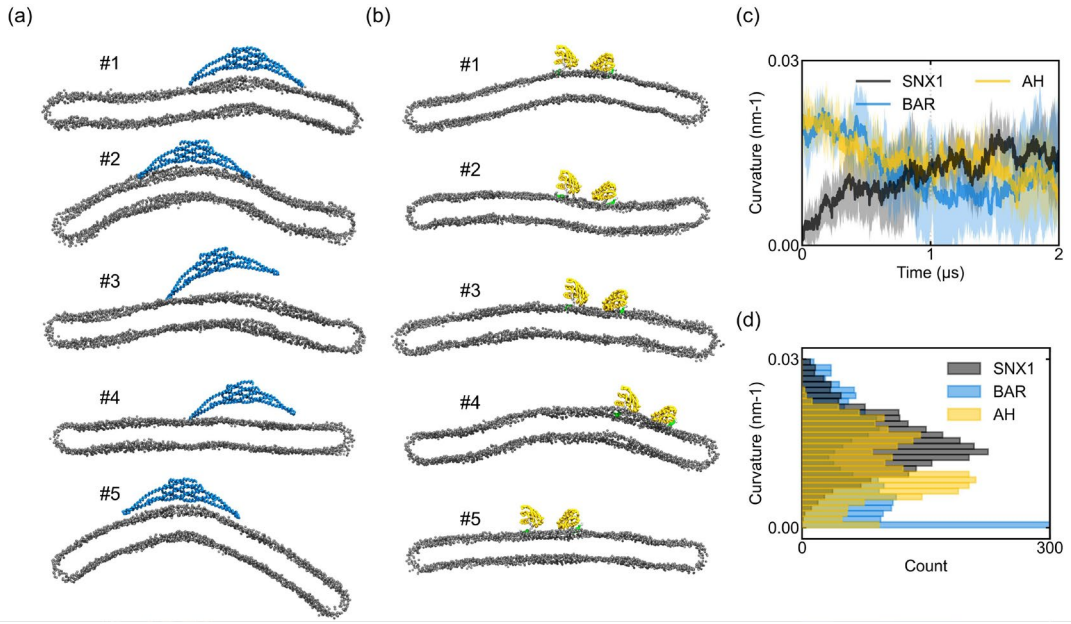

Figure 3. BAR or AH alone fails to maintain the pre-bent membrane. (a) Snapshots of the membrane in the presence of BAR domain from replicas #1 to #5. (b) Snapshots of the membrane in the presence of AH and PX domain from replicas #1 to #5. (c) Time evolution of the mean membrane curvature from five replicas in the systems with the full-length SNX1, BAR and AH domain. The error bar is plotted as a shaded area. (d) Histograms of the membrane curvature for the three systems. It is difficult for BAR or AH to maintain the membrane curvature when acting alone.

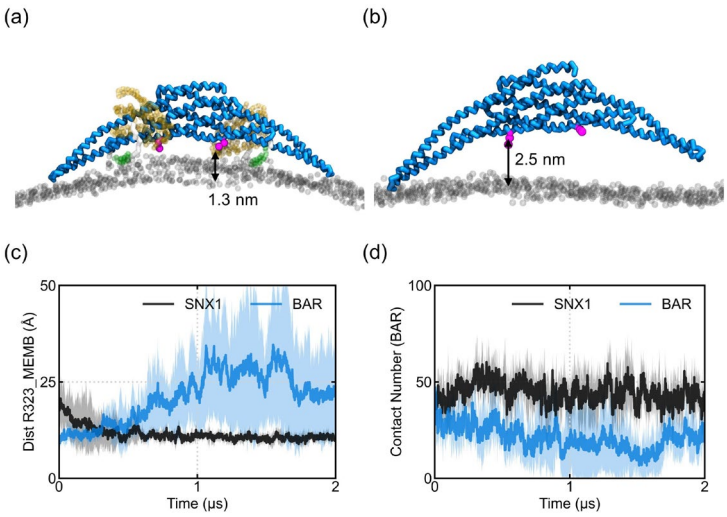

Figure 4. The influence of removing PX and AH on the membrane conformation of BAR domain. The conformation of BAR domain on the membrane in the (a) SNX1 and (b) BAR-only system. Residues R323 at the top of the concave surface of BAR domain are represented as magenta spheres. (c) A time series of the distance between R323 and the membrane. (d) Time course of the contact number between the BAR domain and the membrane. The membrane becomes flatter in the BAR-only system due to the weakened interaction between lipids and the curved region.

We conducted further analysis to explain why BAR or AH alone faces difficulty in maintaining the membrane curvature. Contact analysis indicates that there are some differences in the PI3P binding site in the BAR-only system compared to the SNX1 system (Figure S9a and b). Upon removal of AH and PX, less PI3P is attracted to the upper region of the concave surface of BAR (around residue 323). We speculated that the distance from the top of the concave surface to the membrane is related to the ability of membrane remodeling. The distance from R323 to the membrane was calculated to evaluate the separation between the concave surface and the membrane (Figure 4a-c). The distance is only 1.3 nm in the complete SNX1 system. In the BAR-only system, the concave surface of the BAR domain moves away from the membrane, with a distance of 2.5 nm. The average contact number between BAR domain and lipids is only half of that in the SNX1 system (Figure 4d). The analysis indicates that when AH and PX are removed, lipids struggle to absorb to the top of the concave surface, leading to the reduction of contact. The weakened interaction between BAR and lipids makes it difficult to remodel the membrane through the scaffolding mechanism.

Then, we explored the impact of removing BAR on the membrane interaction of PX and AH. The PI3P contact analysis reveals that the removal of the BAR domain results in more contact between AH and PI3P lipids (Figure S9c and d). AH penetrates the membrane more deeply and establishes greater lipid interactions, which may be attributed to the removal of the steric hindrance imposed by BAR domain (Figure S10 a-d). For the PX domain, the removal of the BAR domain leads to more PI3P contacts

with Residues K195, K199 and Q202, and fewer contacts with K220 and K225 (Figure S9c and d). Despite PX adopting a different conformation relative to the membrane, the contact number of PX domain with lipids remains unchanged (Figure S10e). These results suggest that the removal of the BAR domain leads to conformational changes of PX and AH on the membrane. However, despite AH penetrating more deeply, it remains challenging to maintain membrane curvature in the absence of the BAR domain.

3. PI3P is essential for SNX1-mediated membrane bending

PI3P lipids play a crucial role in membrane localization of PX and SNX proteins.[12, 18] To investigate the influence of PI3P on the membrane bending of SNX1, we modeled a zwitterionic (PC) membrane and an anionic (0.4PC/0.3PE/0.3PS) membrane without PI3P, and then conducted simulations of these membranes interacting with the full-length SNX1. In the PC simulations, SNX1 cannot remodel the PC membrane (Figure 5a, S11a and Video S5). Simulation snapshots show that SNX1 is not even bound to PC lipids, indicating that the electrostatic interactions generated by charged lipids are crucial for membrane binding and bending. In the simulations where PI3P was replaced by PS (denoted as PS simulations), membranes in replicas #1 and #3 are bent, whereas others remain flat (Figure 5b, S11b and Video S6). The membrane curvature as a function of time presents that the PC membrane remains flat under the interaction with SNX1 (Figure 5c). In the PS system, although the avearge membrane curvature

gradually increases and reaches the value comparable to that in the SNX1 system, the histogram shows that most PS membranes have a curvature of 0 nm^{-1} (Figure 5d). The high average membrane curvature in the PS system is due to some of the replicas exhibiting high membrane curvature, such as a curvature of 0.04 nm^{-1} in replica #3. Statistical analysis reveals a statistically significant difference in membrane curvature between the PS system and the SNX1 system (see SI-2 in Supporting Information). Moreover, the calculation of contact number indicates that replacing PI3P with PS results in a reduction in membrane contact in all three regions of SNX1, making membrane binding and bending more challenging (Figure S12). These results show that the presence of PI3P is crucial for SNX1 to induce membrane curvature.

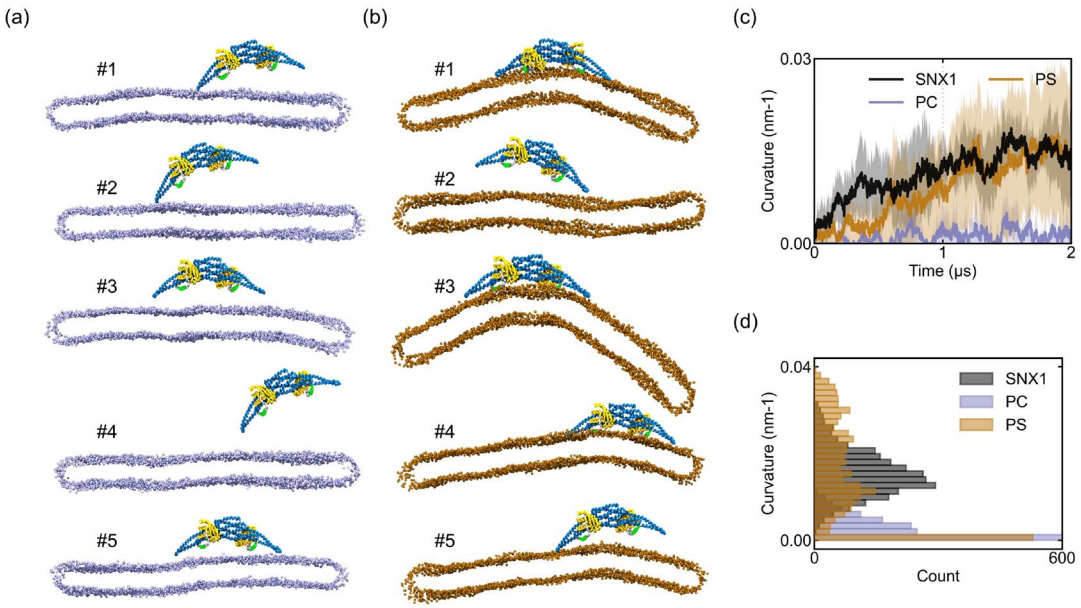

Figure 5. SNX1 finds it difficult to induce membrane remodeling in the absence of PI3P. (a) Snapshots of the SNX1 protein on the PC membrane from replicas #1 to #5. (b) Snapshots of the SNX1 protein on the PS membrane from replicas #1 to #5. (c)

Time evolution of the average membrane curvature from five replicas in the systems of SNX1, PC and PS. (d) Histograms of the membrane curvature in the three systems.

To distinguish the roles of different lipids in the interactions with SNX1, the distribution of lipids around SNX1 was characterized by lipid contact and RDF. In the SNX1 system, SNX1 aggregates more negatively charged lipids (PI3P and DOPS) than uncharged lipids (DOPC and DOPE), validating that the charged lipids are attracted by SNX1 and involved in the scaffolding mechanism (Figure 6a and b). The preference for PI3P is significantly greater than DOPS, indicating the dominant role of PI3P lipids in the interactions with SNX1. In the PS system, PS lipids are unable to form clusters to the same extent as PI3P in the SNX1 system, emphasizing the unique role of PI3P (Figure 6c and d). Since both PI3P and DOPS participate in the electrostatic interactions for the scaffolding mechanisms, the interaction energy between lipids and the BAR domain was calculated to evaluate the role of charged lipids in the scaffolding mechanism (Figure 6e and f). The number of charged lipids in the SNX1 system is equivalent to that in the PS system. However, the interaction energy between charged lipids and the BAR domain in the SNX1 system is -405.4 kJ/mol, much larger than the -169.1 kJ/mol for the PS system. When decomposing the interaction energy for the SNX1 system into contributions from PI3P and DOPS, we observed that PI3P, constituting 10% of all lipids, exhibits an interaction energy of -264.5 KJ/mol, while DOPS, making up 20% of all lipids and being twice the quantity of PI3P, only yields an interaction energy of -140.8 KJ/mol. The comparison of interaction energies

suggests that PI3P lipids produce much stronger interactions with BAR domain of SNX1 than DOPS. The absence of PI3P significantly weakens the interaction between BAR and the membrane, making SNX1 difficult to remodel the membrane through the scaffolding mechanism.

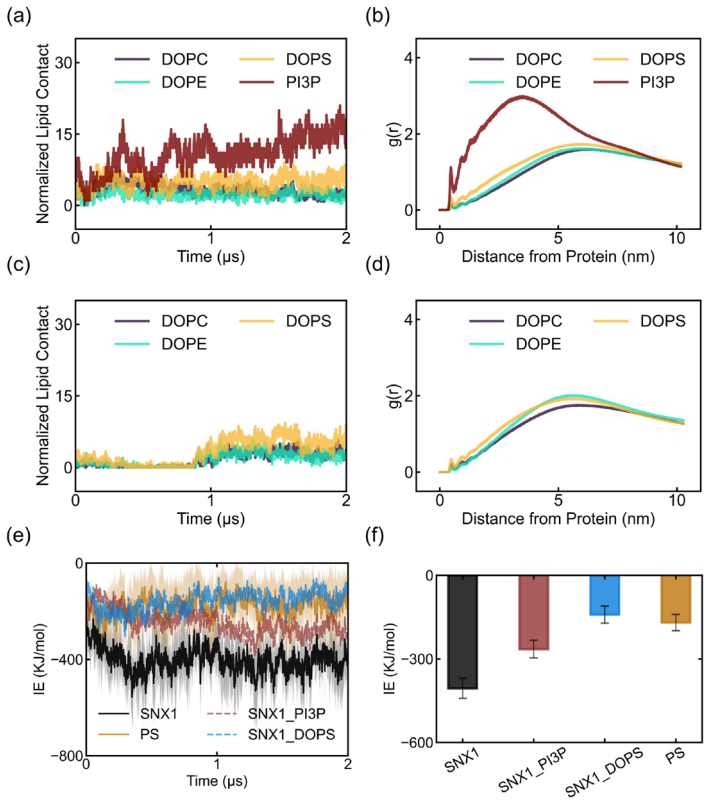

Figure 6. Role of PI3P in the membrane bending of SNX1. (a) Normalized lipid contact as a function of time in the SNX1 system. Lipids within 5.5 Å of SNX1 are considered as contact lipids. The contact lipids are counted and then normalized by the proportion of the corresponding lipids in the membrane. (b) RDF of four types of lipids around the protein in the SNX1 system. (c) Normalized lipid contact as a function of time and (d) RDF of lipids around the protein in the PS system. (e) Interaction energy as a function of time and (f) the averaged interaction energy over the last 0.2 μs simulation, between

charged lipids and the BAR domain in the SNX1 and PS systems. SNX1 and PS represent the interactions between all charged lipids and BAR domain in the SNX1 and PS system, respectively. SNX1_PI3P and SNX1_DOPS correspond to the interactions of BAR domain with PI3P and DOPS lipids in the SNX1 system. PI3P lipids form clusters around SNX1 and play a key role in the interactions between lipids and the BAR domain.

Discussion

Our simulations provide insights into the dynamic process of SNX1 remodeling the membrane, elucidate the mechanism in driving membrane curvature, and assess the role of lipids in membrane perturbation. Results obtained here are in line with a recent experimental study of SNX1.[21] First, SNX1 homodimer can induce a curvature of 0.025 nm^{-1} on the membrane, with a radius of 40 nm. The radius is consistent with the diameters of the membrane tubules under the SNX1 lattice (around 40 nm). While in some of the replicates, SNX1 produced a flatter membrane compared to the experiment, with a curvature of 0.015 nm^{-1}. Since in the experiment SNX1 assembles into a protein lattice, this suggests that the protein-protein interactions in the lattice may further promote membrane remodeling. Moreover, the membrane conformation of SNX1 obtained from our simulations is consistent with that in the Cryo-EM structure of SNX1. The concave surface of BAR is closely associated with the membrane, while AH in the linker region between PX and BAR domains appears to be buried in the membrane. Our results also demonstrate that the latest Martini 3 force field is suitable for membrane ribbon simulation and describing the membrane remodeling process.

Our simulations clarify the role of PX, BAR and AH in the SNX1-induced membrane curvature. Our simulation results indicate that all three domains work together to achieve membrane deformation, and BAR or AH is unable to drive the membrane curvature when acting alone. These findings are in accordance with the experiments that all three structural regions contribute to the generation of membrane curvature.[18,

[21] Our simulations deepen the understanding of the role of BAR in the membrane remodeling of SNX1. On the one hand, we identified that multiple negatively charged residues (R323, R406, R418, K428 and K429) on the concave side of BAR interact electrostatically with PI3P lipids. This suggests that BAR domain of SNX1 is capable of remodeling the membrane through scaffolding mechanism. On the other hand, The BAR domain struggles to bind to the membrane through the concave surface and perturb the membrane in the absence of AH and PX, which explains why mutating residues on PX or AH in the experiment reduces the ability of SNX1 to induce membrane curvature.[21] The BAR domain of SNX1 requires membrane-binding regions like PX or AH to achieve membrane perturbation, representing a unique mechanism within BAR protein family. In N-BAR proteins, the BAR domain can independently induce membrane curvature, because it is more rigid and exhibits higher intrinsic curvature.[22-24, 48] In PH-BAR proteins, despite the presence of a phosphoinositide-binding domain PH similar to PX, the BAR domain does not directly participate in the membrane deformation.[49] These findings remind researchers to carefully investigate the bending mechanism of each protein in the BAR protein family.

The helix insertion mechanism also occurs in the SNX1-mediated membrane bending. In the full-length SNX1 system, AH penetrates into the membrane and produces strong interactions with lipids. When the BAR domain is removed, AH can still maintain membrane curvature in replicas #1 and #3. These results indicate that AH also contributes to membrane bending, corresponding to the experimental results that

AH is crucial for membrane remodeling.[17, 18, 21] However, in most replicas of the AH-only systems, AH fails to maintain the membrane bending, suggesting that only helix insertion mechanism is not sufficient to drive membrane bending and requires a combined action with the scaffolding mechanism. The inability of AH to independently induce membrane curvature may be due to its low concentration. Previous simulations have suggested that AH alone in other BAR proteins can produce membrane curvature at higher AH/lipid ratios.[23, 24] Therefore, the impact of AH concentration on membrane bending needs to be analyzed in future studies.

Our results also indicate that PI3P plays a unique role in the membrane bending of SNX1. PI3P lipids enhance the membrane binding and remodeling of SNX1, while SNX1 promotes the local clustering of the neighboring PI3P lipids. These results are consistent with the experimental evidence that SNX1 associates with endosomes through PI3P.[26] As PI3P is enriched in the early endosomes, it can be inferred that SNX1 has the ability to recognize distinct endosomal subdomains and sense membrane curvature through its specific binding to PI3P.[9] PI3P clustering also promotes more SNX1 proteins to cluster, forming oligomers or lattices to generate a greater curvature. Our simulation results indicate that the PI3P-specific binding of SNX1 is mainly attributed to electrostatic attraction. It is evident that PI3P has the highest charge in the endosomal membrane used in this study, thus dominating SNX1-induced membrane curvature. When it is replaced by an equal amount of PS lipids, the total charge decreases, weakening the scaffolding mechanism and making membrane curvature

more challenging. Therefore, we believe there is a threshold for the total charge of lipids to achieve stable membrane curvature, and this threshold is mainly determined by the types and quantities of charged lipids in the membrane. Moreover, our simulations show that PI3P is not bound to the canonical PI3P binding site of the PX domain. It is likely that the membrane ribbon is more dynamics than the simple periodic membrane, making it difficult for lipids to enter the binding site. However, we observed that PI3P can strongly interact with the positively charged residues on the concave surface of BAR domain, acting a dominant role in the scaffolding mechanism. This suggests that PI3P is not only involved in the specific binding to PX for membrane association but is also indispensable for membrane perturbation.

Conclusions

In summary, we have gained molecular insights into how the SNX1 proteins promote membrane curvature on the endosomal membrane through coarse-grained MD simulations. SNX1 can induce membrane curvature through the cooperation of PX, AH and BAR domain. The BAR domain of SNX1 can remodel the membrane through the scaffolding mechanism, but it requires PX and AH to ensure its stable binding to the membrane. The insertion of AH promotes the generation of the membrane curvature, but it is not sufficient to maintain membrane bending when acting alone. SNX1 induces the local clustering of PI3P lipids, while PI3P lipids are necessary for membrane remodeling of SNX1. PI3P dominates the electrostatic interactions between lipids and the BAR domain, playing a crucial role in driving membrane remodeling through the scaffolding mechanism. We hope that the data presented here will deepen the understanding of the mechanism of SNX1-induced membrane remodeling, and drive research on the membrane-bending mechanism of other proteins in the SNX protein family.

ASSOCIATED CONTENT

Data Availability

Initial configurations, input parameters, topologies and trajectory are available at https://doi.org/10.5281/zenodo.10432113

Supporting Information

The Supporting Information (SI) is available free of charge at https://pubs.acs.org/doi/xxx.

The structure and model of the SNX1 protein, initial setup, electrostatic potential map, the membrane insertion of AH, the binding pocket of PI3P, normalized contact number and interaction energy, membrane curvature for each replica, results of the curved membrane with no protein, interfaces between PI3P and the protein in the BAR-only and AH-only system, the effect of removing BAR domain on the membrane conformation of PX and AH, statistical analysis, and additional simulation for result validation (PDF)

SI Video S1: Membrane bending process in the SNX1 system (AVI)

SI Video S2: Membrane and BAR domain in the BAR only system (AVI)

SI Video S3: Membrane, AH and PX domain in the AH only system (AVI)

SI Movie S4: The flattening of the curved membrane in the Membrane only system (AVI)

SI Movie S5: SNX1 on the PC membrane (AVI)

SI Movie S6: SNX1 on the PC/PE/PS membrane (AVI)

AUTHOR INFORMATION

Corresponding Authors

Jun Fan − Department of Materials Science and Engineering, Department of Mechanical Engineering, and Centre for Advanced Nuclear Safety and Sustainable Development, City University of Hong Kong, Kowloon 999077, Hong Kong, China; orcid.org/0000-0001-8227-9671; Email: junfan@cityu.edu.hk

Authors

Zhenyu Liao − Department of Materials Science and Engineering, City University of Hong Kong, Kowloon 999077, Hong Kong, China; orcid.org/0000-0001-9500-3420; Email: zhenyliao4-c@my.cityu.edu.hk

Ting Si - Department of Materials Science and Engineering and Department of Physics, City University of Hong Kong, Kowloon 999077, Hong Kong, China; orcid.org/0000-0002-4291-9205; Email: tingsi2-c@my.cityu.edu.hk

Ji-Jung Kai - Department of Mechanical Engineering and Centre for Advanced Nuclear Safety and Sustainable Development, City University of Hong Kong, Kowloon 999077, Hong Kong, China; orcid.org/0000-0001-7848-8753; Email: jijkai@cityu.edu.hk

Complete contact information is available at:

https://pubs.acs.org/doi/xxx

Author Contributions

Z. L. designed and carried out the simulations and the analysis. J. F. supervised the research. All the authors contributed to the discussion, writing and revising of the manuscript.

Notes

The authors declare no competing financial interests.

ACKNOWLEDGMENTS

This work was supported by the Research Grants Council of Hong Kong (CityU 11305919 and 11308620) and NSFC/RGC Joint Research Scheme N_CityU104/19. Hong Kong Research Grant Council Collaborative Research Fund: C1002-21G and C1017-22G. This research made use of the computing resources of the X-GPU cluster supported by the Hong Kong Research Grant Council Collaborative Research Fund: C6021-19EF.

Reference

(1) Cui, L.; Li, H.; Xi, Y.; Hu, Q.; Liu, H.; Fan, J.; Xiang, Y.; Zhang, X.; Shui, W.; Lai, Y. Vesicle trafficking and vesicle fusion: mechanisms, biological functions, and their implications for potential disease therapy. *Mol. Biomed.* **2022**, *3*, 29.

(2) Bonifacino, J. S.; Glick, B. S. The Mechanisms of Vesicle Budding and Fusion. *Cell* **2004**, *116*, 153-166.

(3) Mehrani, A.; Stagg, S. M. Probing intracellular vesicle trafficking and membrane remodelling by cryo-EM. *J. Struct. Biol.* **2022**, *214*, 107836.

(4) Vieira, N.; Rito, T.; Correia-Neves, M.; Sousa, N. Sorting Out Sorting Nexins Functions in the Nervous System in Health and Disease. *Mol. Neurobiol.* **2021**, *58*, 4070-4106.

(5) Yang, J.; Villar, Van Anthony M.; Rozyyev, S.; Jose, Pedro A.; Zeng, C. The emerging role of sorting nexins in cardiovascular diseases. *Clin. Sci.* **2019**, *133*, 723-737.

(6) Zhang, H.; Huang, T.; Hong, Y.; Yang, W.; Zhang, X.; Luo, H.; Xu, H.; Wang, X. The Retromer Complex and Sorting Nexins in Neurodegenerative Diseases. *Front. Aging Neurosci.* **2018**, *10*, 79.

(7) Huang, J.; Tiu, A. C.; Jose, P. A.; Yang, J. Sorting nexins: role in the regulation of blood pressure. *FEBS J.* **2023**, *290*, 600-619.

(8) Yang, L.; Tan, W.; Yang, X.; You, Y.; Wang, J.; Wen, G.; Zhong, J. Sorting nexins: A novel promising therapy target for cancerous/neoplastic diseases. *J. Cell. Physiol.* **2021**, *236*, 3317-3335.

(9) Cullen, P. J. Endosomal sorting and signalling: an emerging role for sorting nexins. *Nat. Rev. Mol. Cell Biol.* **2008**, *9*, 574-582.

(10) Teasdale, Rohan D.; Collins, Brett M. Insights into the PX (phox-homology) domain and SNX (sorting nexin) protein families: structures, functions and roles in disease. *Biochem. J* **2011**, *441*, 39-59.

(11) Seet, L.-F.; Hong, W. The Phox (PX) domain proteins and membrane traffic. *Biochim. Biophys. Acta - Mol. Cell Biol. Lipids.* **2006**, *1761*, 878-896.

(12) Chandra, M.; Chin, Y. K. Y.; Mas, C.; Feathers, J. R.; Paul, B.; Datta, S.; Chen, K.; Jia, X.; Yang, Z.; Norwood, S. J.; et al. Classification of the human phox homology (PX) domains based on their phosphoinositide binding specificities. *Nat. Commun.* **2019**, *10*, 1528.

(13) West, A.; Brummel, B. E.; Braun, A. R.; Rhoades, E.; Sachs, J. N. Membrane remodeling and mechanics: Experiments and simulations of α-Synuclein. *Biochim. Biophys. Acta, Biomembr.* **2016**, *1858*, 1594-1609.

(14) Chan, C.; Wen, H.; Lu, L.; Fan, J. Multiscale molecular dynamics simulations of membrane remodeling by Bin/Amphiphysin/Rvs family proteins*. *Chin. Phys. B* **2016**, *25*, 018707.

(15) Peter, B. J.; Kent, H. M.; Mills, I. G.; Vallis, Y.; Butler, P. J. G.; Evans, P. R.; McMahon, H. T. BAR Domains as Sensors of Membrane Curvature: The Amphiphysin BAR Structure. *Science* **2004**, *303*, 495-499.

(16) Frost, A.; Perera, R.; Roux, A.; Spasov, K.; Destaing, O.; Egelman, E. H.; De Camilli, P.; Unger, V. M. Structural Basis of Membrane Invagination by F-BAR Domains. *Cell* **2008**, *132*, 807-817.

(17) van Weering, J. R. T.; Sessions, R. B.; Traer, C. J.; Kloer, D. P.; Bhatia, V. K.; Stamou, D.; Carlsson, S. R.; Hurley, J. H.; Cullen, P. J. Molecular basis for SNX-BAR-mediated assembly of distinct endosomal sorting tubules. *EMBO J.* **2012**, *31*, 4466-4480.

(18) Pylypenko, O.; Lundmark, R.; Rasmuson, E.; Carlsson, S. R.; Rak, A. The PX-BAR membrane-remodeling unit of sorting nexin 9. *EMBO J.* **2007**, *26*, 4788-4800.

(19) Gallop, J. L.; Jao, C. C.; Kent, H. M.; Butler, P. J. G.; Evans, P. R.; Langen, R.; McMahon, H. T. Mechanism of endophilin N-BAR domain-mediated membrane curvature. *EMBO J.* **2006**, *25*, 2898-2910.

(20) Campelo, F.; McMahon, H. T.; Kozlov, M. M. The Hydrophobic Insertion Mechanism of Membrane Curvature Generation by Proteins. *Biophys. J.* **2008**, *95*, 2325-2339.

(21) Zhang, Y.; Pang, X.; Li, J.; Xu, J.; Hsu, V. W.; Sun, F. Structural insights into membrane remodeling by SNX1. *Proc. Natl. Acad. Sci. U.S.A.* **2021**, *118*, e2022614118.

(22) Chen, Z.; Zhu, C.; Kuo, C. J.; Robustelli, J.; Baumgart, T. The N-Terminal Amphipathic Helix of Endophilin Does Not Contribute to Its Molecular Curvature Generation Capacity. *J. Am. Chem. Soc.* **2016**, *138*, 14616-14622.

(23) Arkhipov, A.; Yin, Y.; Schulten, K. Membrane-Bending Mechanism of Amphiphysin N-BAR Domains. *Biophys. J.* **2009**, *97*, 2727-2735.

(24) Blood, P. D.; Swenson, R. D.; Voth, G. A. Factors Influencing Local Membrane Curvature Induction by N-BAR Domains as Revealed by Molecular Dynamics Simulations. *Biophys. J.* **2008**, *95*, 1866-1876.

(25) van Weering, J. R. T.; Verkade, P.; Cullen, P. J. SNX–BAR proteins in phosphoinositide-mediated, tubular-based endosomal sorting. *Semin. Cell Dev. Biol.* **2010**, *21*, 371-380.

(26) Carlton, J.; Bujny, M.; Peter, B. J.; Oorschot, V. M. J.; Rutherford, A.; Mellor, H.; Klumperman, J.; McMahon, H. T.; Cullen, P. J. Sorting Nexin-1 Mediates Tubular Endosome-to-TGN Transport through Coincidence Sensing of High- Curvature Membranes and 3-Phosphoinositides. *Curr. Biol.* **2004**, *14*, 1791-1800.

(27) Larsen, A. H. Molecular Dynamics Simulations of Curved Lipid Membranes. *Int. J. Mol. Sci.* **2022**, *23*, 8098.

(28) Guo, J.; Bao, Y.; Li, M.; Li, S.; Xi, L.; Xin, P.; Wu, L.; Liu, H.; Mu, Y. Application of computational approaches in biomembranes: From structure to function. *WIREs Comput. Mol. Sci.* **2023**, *13*, e1679.

(29) Mahmood, M. I.; Noguchi, H.; Okazaki, K.-i. Curvature induction and sensing of the F-BAR protein Pacsin1 on lipid membranes via molecular dynamics simulations. *Sci. Rep.* **2019**, *9*, 14557.

(30) Mahmood, M. I.; Poma, A. B.; Okazaki, K.-i. Optimizing Gō-MARTINI Coarse-Grained Model for F-BAR Protein on Lipid Membrane. *Front. Mol. Biosci.* **2021**, *8*, 619381.

(31) Belessiotis-Richards, A.; Higgins, S. G.; Sansom, M. S. P.; Alexander-Katz, A.; Stevens, M. M. Coarse-Grained Simulations Suggest the Epsin N-Terminal Homology Domain Can Sense Membrane Curvature without Its Terminal Amphipathic Helix. *ACS Nano* **2020**, *14*, 16919-16928.

(32) Mandal, T.; Spagnolie, S. E.; Audhya, A.; Cui, Q. Protein-induced membrane curvature in coarse-grained simulations. *Biophys. J.* **2021**, *120*, 3211-3221.

(33) Bhaskara, R. M.; Grumati, P.; Garcia-Pardo, J.; Kalayil, S.; Covarrubias-Pinto, A.; Chen, W.; Kudryashev, M.; Dikic, I.; Hummer, G. Curvature induction and membrane remodeling by FAM134B reticulon homology domain assist selective ER-phagy. *Nat. Commun.* **2019**, *10*, 2370.

(34) Poudel, K. R.; Dong, Y.; Yu, H.; Su, A.; Ho, T.; Liu, Y.; Schulten, K.; Bai, J. A time course of orchestrated endophilin action in sensing, bending, and stabilizing curved membranes. *Mol. Biol. Cell* **2016**, *27*, 2119-2132.

(35) Abraham, M. J.; Murtola, T.; Schulz, R.; Páll, S.; Smith, J. C.; Hess, B.; Lindahl, E. GROMACS: High performance molecular simulations through multi-level parallelism from laptops to supercomputers. *SoftwareX* **2015**, *1-2*, 19-25.

(36) Souza, P. C. T.; Alessandri, R.; Barnoud, J.; Thallmair, S.; Faustino, I.; Grünewald, F.; Patmanidis, I.; Abdizadeh, H.; Bruininks, B. M. H.; Wassenaar, T. A.; et al. Martini 3: a general purpose force field for coarse-grained molecular dynamics. *Nat. Methods* **2021**, *18*, 382-388.

(37) Kroon, P. C.; Grunewald, F.; Barnoud, J.; van Tilburg, M.; Souza, P. C. T.; Wassenaar, T. A.; Marrink, S. J. Martinize2 and Vermouth: Unified Framework for Topology Generation. *eLife* **2023**, *12*, RP90627.

(38) Wassenaar, T. A.; Ingólfsson, H. I.; Böckmann, R. A.; Tieleman, D. P.; Marrink, S. J. Computational Lipidomics with insane: A Versatile Tool for Generating Custom Membranes for Molecular Simulations. *J. Chem. Theory Comput.* **2015**, *11*, 2144-2155.

(39) Borges-Araújo, L.; Souza, P. C. T.; Fernandes, F.; Melo, M. N. Improved Parameterization of Phosphatidylinositide Lipid Headgroups for the Martini 3 Coarse-Grain Force Field. *J. Chem. Theory Comput.* **2022**, *18*, 357-373.

(40) Pannuzzo, M.; Raudino, A.; Böckmann, R. A. Peptide-induced membrane curvature in edge-stabilized open bilayers: A theoretical and molecular dynamics study. *J. Chem. Phys.* **2014**, *141*, 024901.

(41) Wu, Z.; Schulten, K. Synaptotagmin's Role in Neurotransmitter Release Likely Involves Ca2+-induced Conformational Transition. *Biophys. J.* **2014**, *107*, 1156-1166.

(42) Paul, S.; Audhya, A.; Cui, Q. Molecular mechanism of GTP binding- and dimerization-induced enhancement of Sar1-mediated membrane remodeling. *Proc. Natl. Acad. Sci. U.S.A.* **2023**, *120*, e2212513120.

(43) Bussi, G.; Donadio, D.; Parrinello, M. Canonical sampling through velocity rescaling. *J. Chem. Phys.* **2007**, *126*, 014101.

(44) Parrinello, M.; Rahman, A. Polymorphic transitions in single crystals: A new molecular dynamics method. *J. Appl. Phys.* **1981**, *52*, 7182-7190.

(45) Humphrey, W.; Dalke, A.; Schulten, K. VMD: Visual molecular dynamics. *J. Mol. Graphics* **1996**, *14*, 33-38.

(46) Yin, Y.; Arkhipov, A.; Schulten, K. Simulations of Membrane Tubulation by Lattices of Amphiphysin N-BAR Domains. *Structure* **2009**, *17*, 882-892.

(47) Hsin, J.; Gumbart, J.; Trabuco, L. G.; Villa, E.; Qian, P.; Hunter, C. N.; Schulten, K. Protein-Induced Membrane Curvature Investigated through Molecular Dynamics Flexible Fitting. *Biophys. J.* **2009**, *97*, 321-329.

(48) Salzer, U.; Kostan, J.; Djinović-Carugo, K. Deciphering the BAR code of membrane modulators. *Cell. Mol. Life Sci.* **2017**, *74*, 2413-2438.

(49) Pang, X.; Fan, J.; Zhang, Y.; Zhang, K.; Gao, B.; Ma, J.; Li, J.; Deng, Y.; Zhou, Q.; Egelman, Edward H.; et al. A PH Domain in ACAP1 Possesses Key Features of the BAR Domain in Promoting Membrane Curvature. *Dev. Cell* **2014**, *31*, 73-86.

TOC GRAPHICS